Recuperación mejorada como resultado de la inducción de ondas

Mario Ubaldo Rangel
José Emilio Santamaría Díaz
Reynaldo Bautista Morales
Rafael Santamaría Díaz
Fernando Samaniego Verduzco
UNAM

Artículo recibido en agosto de 2023-evaluado-corregido y aceptado en septiembre de 2023

Resumen

Este trabajo presenta un nuevo modelo acoplado entre la ecuación de difusión y la ecuación de onda para analizar la recuperación mejorada de petróleo (EOR) de pozos en yacimientos. Se presentan experimentos de laboratorio que han validado el modelo. Las ondas que se propagan generadas por este método, a través de las características inherentes del sistema roca-fluido han llevado a modificaciones en las presiones capilares, retención de fluido en los poros, vibraciones de la roca y energía cinética en los fluidos. En consecuencia, estas alteraciones facilitan el flujo de petróleo hacia los pozos productores.

Palabras clave: Ondas inducidas, EOR, yacimiento, frecuencia, estimulación, vibraciones.

Enhanced oil recovery as result of induced waves

Abstract

This paper introduces a new coupled wave and diffusivity pressure equation model to analyze enhanced oil recovery (EOR) from reservoir wells. Laboratory experiments have validated the model. The propagating waves generated by this approach through the inherent characteristics of the rock-fluid system led to modifications in capillary pressures, pore fluid retention, rock vibrations, and kinetic energy in fluids. Consequently, these alterations facilitate the oil flow toward the producing wells.

Keywords: Induced waves, EOR, reservoir, frequency, stimulation, vibrations.

Introduction

Throughout the history of the petroleum industry induced waves have found various applications, including prospecting and pulse testing. Pulse testing involves the generation of induced waves (IW) within petroleum reservoirs through variations in flow rate and pressure changes. These induced waves create pseudo waves or pressure wave displacement through the porous media.

When induced pressure waves propagate through the reservoir, their movement is influenced by the radius of the investigation and their properties. The induced wave displacement within the formation occurs faster than the natural pressure drop wave.

The main objective of this paper is to validate through a coupled model of induced waves and diffusivity pressure equations, laboratory tests. The validation aims to

demonstrate the model's effectiveness in simulating the increased production from wells.

Studies conducted worldwide have examined the effects of seismic waves within reservoirs, with observed increases in hydrocarbon production resulting from the seismic effect. In the 1970s there was a Russian report about increased oil production in a field due to an earthquake, in which the production increased during the event and continued for some time afterward. The report also mentioned a change in water cut, which persisted after the event and drew attention to the phenomenon.

Nikolaevskij (1996) conducted a study examining how both natural and artificial vibro-stimulation influence on relative permeabilities in porous media. Subsequently, in January 1997, a research team led by Davison initiated laboratory testing, **Figure 1**. This endeavor was followed by field tests (in Argentina) that spanned from 1999 to 2001. The objective of their research was the development of a specialized fluid for injection into downhole tools within oil wells. This innovation aimed to enhance oil production in water injection wells, thus bolstering secondary recovery techniques within oil fields.

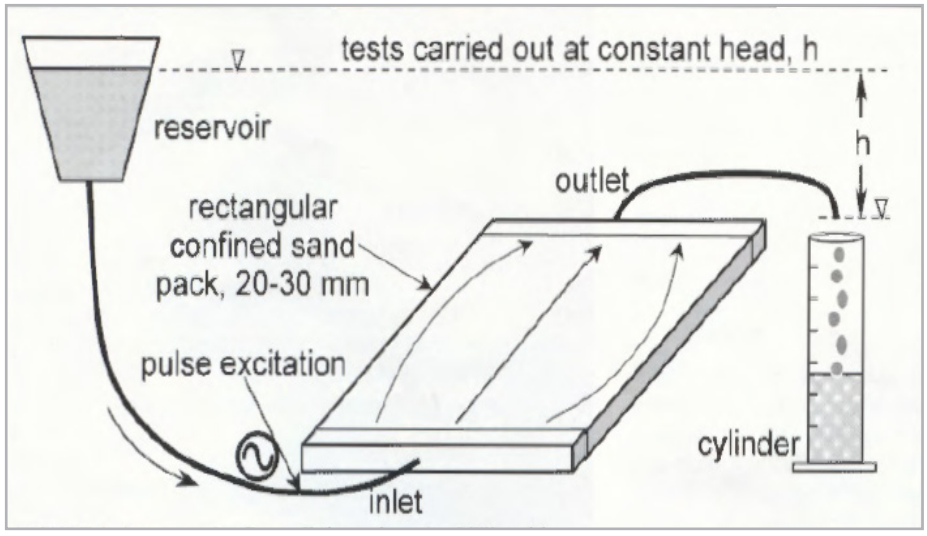

Figure 1. The laboratory experiments were conducted using a confined rectangular sand pack arrangement, where water is injected in pulses. In other words, the injection line serves as the source of waves (pulses) (Dusseault et al., 2000)

Some significant findings from the 150 experiments conducted are (Spanos et al., 2003):

1. Appropriately applied dynamic excitation with the right frequency and magnitude increases flow rate in porous media.
2. There is no change in basic static permeability associated with this effect because the simulation sands are clean, dense, and rigidly held in place.
3. The flow enhancement occurs in single-phase liquid flow (a relative permeability explanation is therefore out of the question).
4. There are clear transient build-up and decay periods in flow rate as pulsing is periodically stopped and restarted.
5. There are concomitant internal changes in pressure distribution, even though the macroscopic external heads remain constant.
6. The presence of free gas suppresses the flow enhancement effect.
7. The effect occurs for all liquids and permeabilities, but of course the lower the intrinsic static permeability the smaller the flow rate increase.

Remarkably, the research conducted by Davison's team led to the conclusion that wave induction, could exclusively be achieved by the hydraulic generation of pulses within the well, coupled with their downhole tool. This approach was deemed the most suitable, as it effectively prevented any

adverse effects on the well's mechanical integrity. In this setup, the injection frequency is hydraulically controlled, transmitting it from the surface to the desired depth. This configuration initiates a wave disturbance that propagates through the fluid and from the fluid into the formation. The primary challenge lies in the significant attenuation of vibrations from the tool's tip within the wellbore, resulting in the loss of a substantial portion of the vibration inside the well. **Figure 2.**

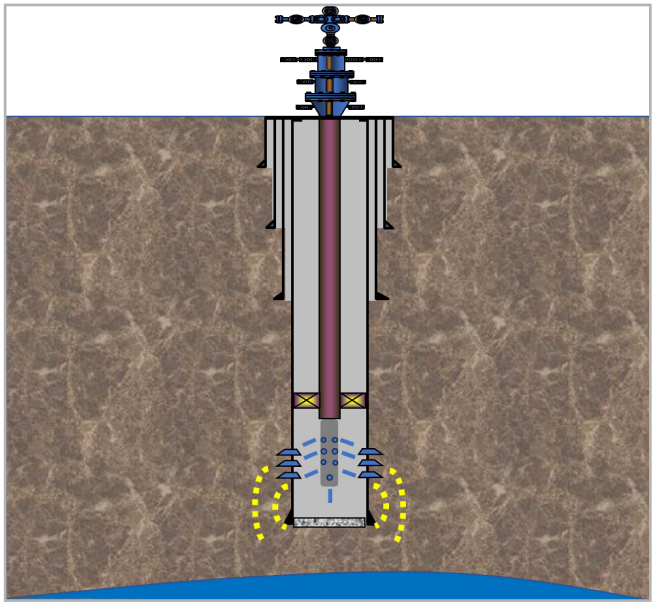

Figure 2. Illustrates the fundamental configuration of pulsatile water injection.

In 2005, Ariadji conducted laboratory experiments, that highlighted frequency as the second most crucial parameter to consider in such investigations.

Recently, Rangel et al. (2020) presented evidence showing that induced mechanical waves can significantly diminish the duration of testing, necessary for studying the characteristics of the formation. This reduction in testing time can be attributed to changes (contraction - dilatation) in porous media by waves. (Geertsma, 1957), (Corapcioglu,1996), (Biot, 1962), (Bear and Corapcioglu, 1989), (Garg, 1971), (Ishihara et al.,1981), (Madsen, 1978), (Mynett,1983), (Nikolaevskihe formationl., 1996), and (Richart et al., 1970). Specifically, the waves introduce energy into the system through vibrational forces. It is crucial to emphasize that these vibrations are generated by a mechanical device, as opposed to being pulse-driven (injection fluid), **Figure 3.**

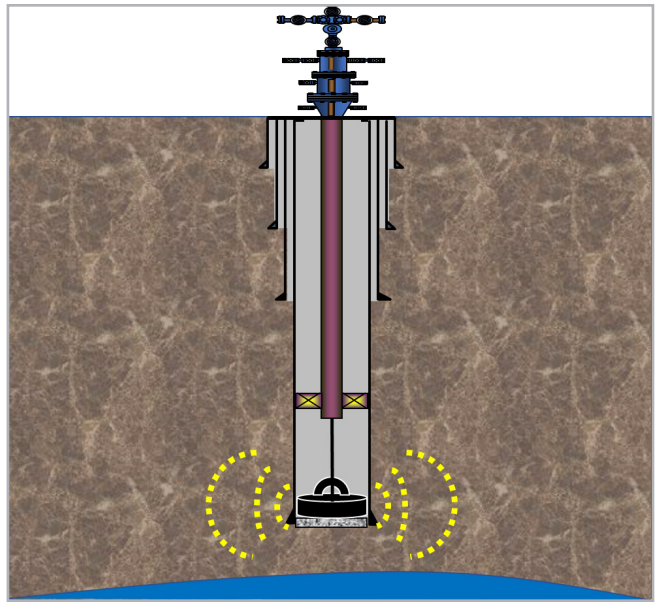

Figure 3. Waves are induced through a device temporarily anchored to the wellbore walls as the source of vibration to propagate through the porous medium (Rangel et al., 2022).

Chen et al. (2020) investigated vibro-stimulation as an enhanced oil recovery (EOR) method, using modified Maxwell's equations to model the reservoir system. However, it is crucial to consider the rock-fluid-pressure drop system to accurately represent the process.

Development

An analysis using the solutions for the wave's displacement through the porous media is presented. The mathematical model is based on the momentum balance equation for the formation and its saturating fluid, Eqs. 1 and 2 (Bear, 2018):

$$(1-\phi)\rho_s \frac{\partial^2 w_{si}}{\partial t^2} - \frac{\partial \sigma_{sji}}{\partial x_j} - (1-\phi)\left[\frac{\partial p}{\partial x_i} + \rho_s g \frac{\partial z}{\partial x_i}\right] - \mu\phi^2 \left(k_{il}\right)^T \frac{\partial}{\partial t}\left(w_{fl} - w_{sl}\right) = 0 \qquad (1)$$

$$(\phi)\rho_f \frac{\partial^2 w_{fi}}{\partial t^2} + (\phi)\left[\frac{\partial p}{\partial x_i} + \rho_f g \frac{\partial z}{\partial x_i}\right] - \mu\phi^2 \left(k_{il}\right)^T \frac{\partial}{\partial t}\left(w_{sl} - w_{fl}\right) = 0 \quad (2)$$

The general fluid flow model is given by Eq. 3 (Rangel et al, 2020):

$$\nabla D p_f = -\xi_f \left[\frac{\mu\phi\left(k_{il}\right)^T}{\rho_f} \frac{\partial(wsl - wfl)}{\partial t} - \frac{1}{\rho_f} \nabla p - g\nabla z\right] \quad (3)$$

The general model considering the compressible porous medium is given by Eqs. 4 and 5:

$$\left(\phi - \phi^2\right)\rho_s \frac{\partial^2 w_{si}}{\partial t^2} - \frac{\partial \sigma_{sji}}{\partial x_j} - \sigma(x,y,z,t) \cdot (1 - \phi) - \mu\phi^3 \left(k_{il}\right)^T \frac{\partial}{\partial t}\left(w_{fl} - w_{sl}\right) = 0 \quad (4)$$

$$(\phi)\rho_f \frac{\partial^2 w_{fi}}{\partial t^2} + \sigma(x,y,z,t) - \mu\phi^2 \left(k_{il}\right)^T \frac{\partial}{\partial t}\left(w_{sl} - w_{fl}\right) = 0 \quad (5)$$

The main assumptions for this work are incompressible fluid for linear and radial geometries, see **Appendices A and B**. The dilation of the porous medium has immediate effects on the fluid, and therefore when the fluid expands within the porous medium, the impact of the waves is directly reflected in the flow of the fluid through the porous medium (Bear and Corapcioglu, 1989), and (Dusseault et al., 2000). Hence, it is valid in a model to neglect the dilation of the porous medium and subsequently add its contribution to oil production (rock and fluid dilation). The term "vibratio-permatio" is introduced to describe the effect of mechanical waves (such as seismic waves and non-acoustic mechanical vibration waves) on the porous medium, which contributes to fluid production through the dilation of the rock-fluid system, see **Appendix C**.

Dilation of the rock (Eq. 6) and the fluid (Eq. 7) as a result of wave induction, exclusively considering the term related to wave propagation (Corapcioglu, 1991), are expressed by Eqs. 6 and 7:

$$\epsilon = C_1 \cdot e^{i(\beta + \theta t)} \quad (6)$$

$$e = C_2 \cdot e^{i(\beta + \theta t)} \quad (7)$$

Dilation of the rock (Eq. 8) and the fluid (Eq. 9) considering the term related to wave attenuation:

$$\epsilon = \epsilon_{max} \cdot e^{i(\beta + \theta t)} e^{-(b)} \quad (8)$$

$$e = e_{max} \cdot e^{i(\beta + \theta t)} e^{-(b)} \tag{9}$$

where the attenuation term (Corapcioglu, 1991):

$$b = \frac{\mu_f \cdot \phi^2}{k} \tag{10}$$

and propagation terms (Corapcioglu, 1991):

$$\beta = \frac{\omega}{v} \tag{11}$$

$$\theta = \omega = 2\pi \cdot f \tag{12}$$

Discussion

For a closed reservoir model, the waves displacements in the solid are expressed by Eq.13 and in the fluid Eq. 14, see **Appendix A Eqs. (A.25 and A.26):**

$$U_{Ds} = \sin \omega_D t_D + \frac{4}{\pi} \sum_{1}^{\infty} \frac{{\omega_D}^2}{{\omega_D}^2 - {\beta_n}^2} C_n \cos \beta_n X \left[\sin \omega_D t_D - \frac{\beta_n}{\omega_D} \sin \beta_n t_D\right] \tag{13}$$

$$\begin{aligned} U_{Df} &= N_{UE} \left\{\omega_D N_{WTN} e^{-\frac{t_D}{N_{WTN}}} + \sin \omega_D t_D - \omega_D N_{WTN} \cos \omega_D t_D\right\} \\ &+ \frac{4\omega_D}{\pi} \sum_{1}^{\infty} \frac{(-1)^n}{2n-1} \frac{\cos\left(\frac{2n-1}{2}\right)\pi[1 - X_D]}{{\beta_n}^2 + {\omega_D}^2} \left\{\omega_D N_{UE} \left(\omega_D N_{WTN} e^{-\frac{t_D}{NWT}} + \sin \omega_D t_D \right.\right. \\ &\left. - \omega_D N_{WTN} \cos \omega_D t_D\right) - \frac{N_{WTN} \beta_n}{1 + (\beta_n N_{WTN})^2} (\beta_n N_{WTN} e^{-\frac{t_D}{N_{WTN}}} + \sin \beta_n t_D \\ &\left. - \beta_n N_{WTN} \cos \beta_n t_D)\right\} \end{aligned} \tag{14}$$

The radial model for the above-described conditions is given by Eqs. 15 and 16:

$$\frac{\partial^2 w_{Ds}}{\partial {r_D}^2} + \frac{1}{r_D} \frac{\partial w_{Ds}}{\partial r_D} = \frac{\partial^2 w_{Ds}}{\partial {t_D}^2} + \frac{1}{\eta_{Diw}} \frac{\partial \left(w_{Ds} - w_{Df}\right)}{\partial t_D} \tag{15}$$

$$\frac{\partial^2 w_{Df}}{\partial t_D^{\,2}} = \frac{1}{N_{WTN}} \frac{\partial\left(w_{Df} - w_{Ds}\right)}{\partial t_D} \tag{16}$$

The solid and fluid numerical solutions for Eqs. (15 and 16), are described in **Appendix B** given by Eqs.17 and 18:

Finite differences of wave displacement in the solid:

$$\omega_{Ds}(i,k) = \left(1 - \varphi_4\right)\omega_{Df}(i-1,k+1) - \omega_{Df}(i-1,k) + 2\varphi_4 * \omega_{Df}(i-1,k) - \varphi_4 * \omega_{Df}(i-1,k-1) + \omega_{Ds}(i,k-1) \tag{17}$$

Finite difference of wave displacement in the fluid:

$$\omega_{Df}(i,k) = \left\{ \frac{\omega_{Df}(i+1,k-1)+\omega_{Df}(i-1,k-1)}{2} + \omega_{Ds}(i,k-1) * \left(\frac{\varphi_3}{2} - \varphi_2\right) + \omega_{Ds}(i-1,k-1) * \left(\frac{\varphi_2}{2} - \frac{\varphi_3}{2}\right) + \omega_{Ds}(i-1,k-1) * \left(\frac{\varphi_2}{2} - \frac{\varphi_3}{2}\right) + \omega_{Ds}(i+1,k-1) * \left(\frac{\varphi_2}{2} - \frac{\varphi_1}{2}\right) - \frac{\varphi_1}{2}\left[\omega_{Df}(i-1,k+1) - 2\,\omega_{Ds}(i,k)\right] \right\} \tag{18}$$

The vibratio - permatio effect modifies in a dimension smaller than the final wave propagation in the porous medium, therefore solutions Eqs. 13, 14, 17 and 18 are valid to determine the wave propagation velocity (In the following, we will not differentiate between wave propagation velocity and propagation itself).

The additional production induced by the wave effect can be calculated for a laboratory core using the modified Darcy's law Eq. 19, see **Appendix C Eqs. (C.23 and C.24):**

$$q_{ERFC} = \frac{k}{\mu} \cdot A_T \cdot \sigma \tag{19}$$

Results

The N_{WTN} value determines the scope of waves that can disturb the porous media, See Eq. (A.5); it can be observed that the N_{WTN} value depends on induction time, reservoir length, and wave speed. It can be observed that the reservoir length and speed reached by the wave depend on the nature of the reservoir. The only values that can be modified are induction time and frequency. The induction time and frequency determine the energy supplied to the reservoir and the resonance pattern that can be used to modify the flow of fluids to the well. **Figure 4** shows the behavior of the travel of the induced wave, varying the induction frequency. It can be observed that at higher frequencies the displacement is smaller, yet faster, whereas at lower frequencies the wave's displacement is more significant over a longer period of time. It is evident that the wave travels faster at higher frequencies, while at lower frequencies it covers greater distances. In other words, for its optimal application, one must determine the desired perturbation length or response time.

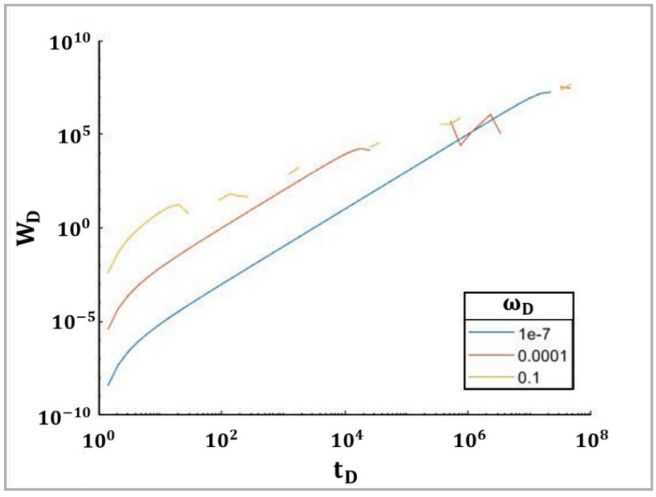

Figure 4. The graph displays three wave displacements within the same porous medium, where only the induction frequency was modified. (Rangel et al, 2020). []

The induction of waves changes the energy of the porous medium concerning effective stress, which in turn enhances fluid flow through the medium, leading to an increase in production. The initial part of this research, which focused on investigating reservoir properties and boundary knowledge through induced wave well-testing, was presented in 2020 by Rangel et al. The subsequent part of the research, which is the focus of this work, will be discussed next.

The vibratio-permatio effect that occurs due to the artificial induction of waves takes place from the well, which is the source, to where the properties of the porous medium allow it, meaning that its effect is attenuated or nullified. In order to determine the velocity of waves within a porous medium, the previously introduced equations (Eqs. 13, 14, 17, and 18) can be used to solve Eqs. 8 and 9. It is essential to understand these equations to improve the flow capacity and spatial extent of the porous medium. **Figure 5** illustrates the dilation-contraction behavior of the medium and its extent (= 0.25, μ_f = 1 [cp], k = 400 [md]).

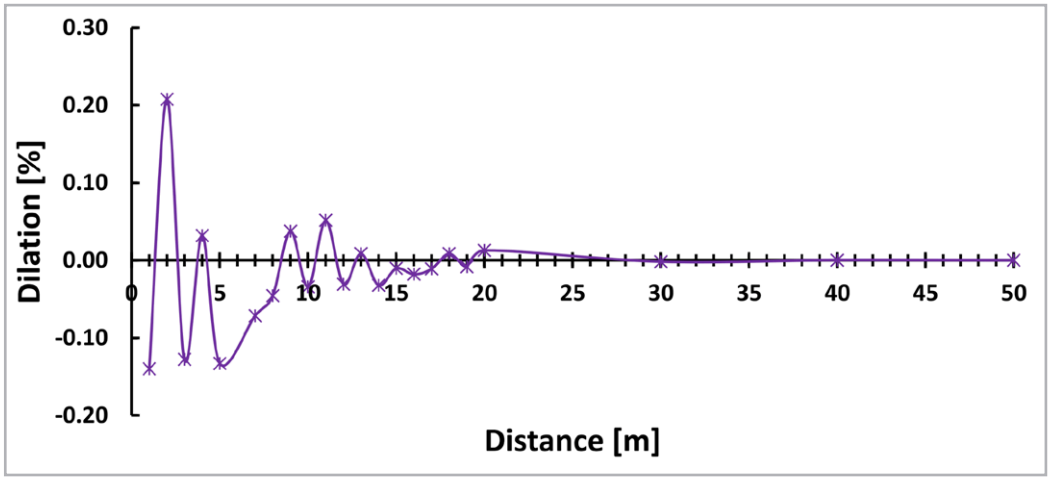

Figure 5. The deformation propagates cyclically through the porous medium with respect to the induction time and attenuates. Notably, it almost entirely attenuates at 30 meters.

The propagation of waves can extend over long distances, as shown in **Figure 6**, where it is evident that the waves attenuate at $r_D = 0.5$ for short times. It should be noted that the study of wave propagation at long times, although the solutions are presented in Appendices A and B, is beyond the scope of this work. The wave oscillates periodically in the porous medium, with the oscillation pattern depending on the induction frequency.

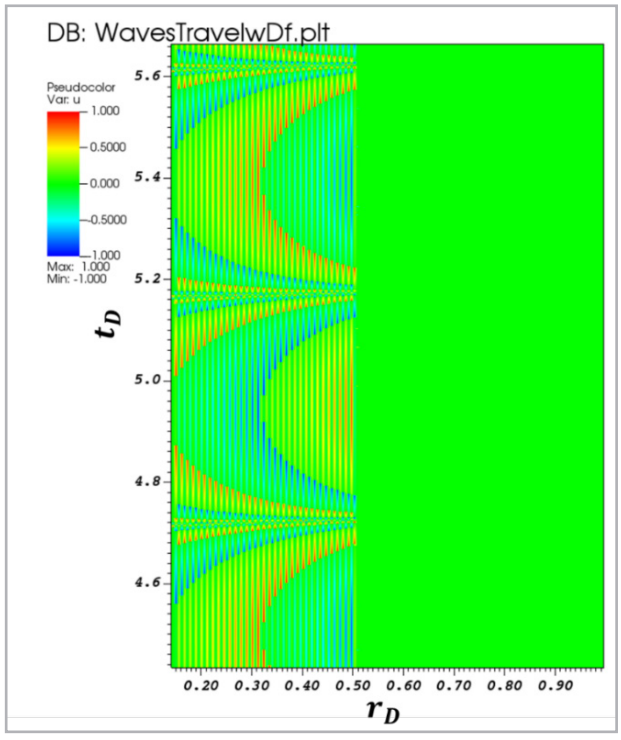

Figure 6. The nature of the waves through porous media with respect to the time, for a wave transmission number $N_{WTN} = 500$, dimensionless frequency $\omega_D = 0.001$, and dimensionless hydraulic diffusivity $\eta_{Diw} = 5$ at, short times.

A detailed view of the wave displacement reveals its behavior, propagation, and attenuation. For an extension of Figure 6, from $r_D = 0$, $t_D = 0$, $r_D = 0.625$ at $t_D = 30$. **Figure 7** illustrates the displacement concerning the traveled distance. Some similarity in displacement behavior can be observed, in contrast to Figure 5, where the deformation caused by the vibratio-permatio effect is evident. This area represents the extent of the wave's reach, and it is essential to note that the area affected by the vibration-permeation effect is smaller than the wave's reach.

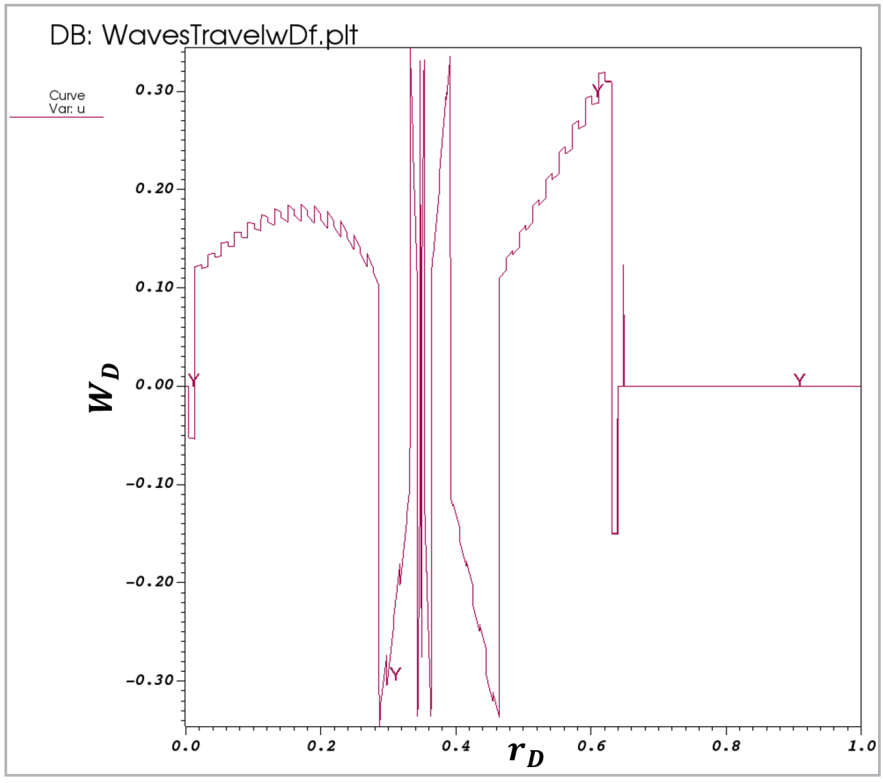

Figure 7. The waves oscillate over time, gradually becoming weaker. The area of displacement, which is up to r_D = 0.625, exhibits cyclical oscillations that affect the porous medium.

A simulation for a reservoir with a radial wave range of 30 [m] was conducted using a laboratory-validated model (explained later), having the following properties: = 0.25, μ_f = 1 [cp], and k = 400 [md]. The simulation showed that the reservoir's flow capacity was enhanced (ERFC) by 1080 [STB/D], indicating an improved fluid contribution of the porous medium. **Figure 8** shows the cumulative production due to the induced waves.

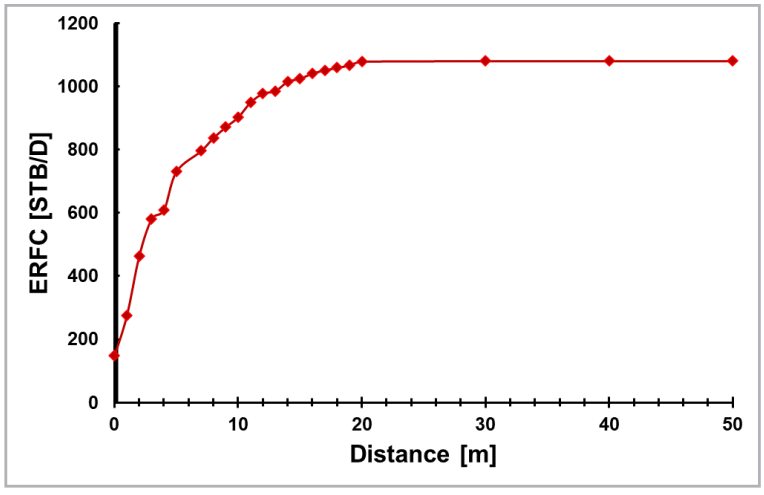

Figure 8. Enhancement of reservoir's flow capacity within first 30 meters from wave source; additional 1080 [STB/D] production was achieved.

Based on the results of the permeability test (last data), it has been determined that if the permeability is less than 100 [md], the ERFC can be considered insignificant, which limits the applicability of this method. On the other hand, when the permeability exceeds 200 [md], the method becomes more feasible, **Figure 9**.

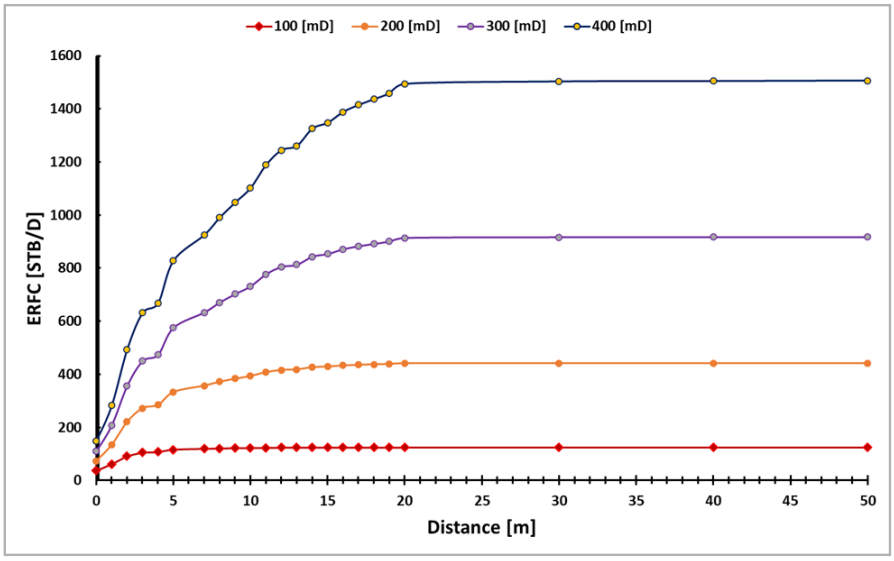

Figure 9. Low permeability values difficult the vibratio-permatio effect, thus rendering its successful implementation contingent upon either high permeability, or as an alternative a low dynamic viscosity.

To understand why the ERFC decreases when permeability is lower, **Figure 10** illustrates a sensitivity study of porous medium dilation concerning its permeability. While a frequency of 350 [Hz] causes deformation of the medium up to 30 [m] for a permeability of 100 [md], the extent wave´s deformation for a permeability of 400 [md] exceeds 50 [m], resulting in a more significant flow increase.

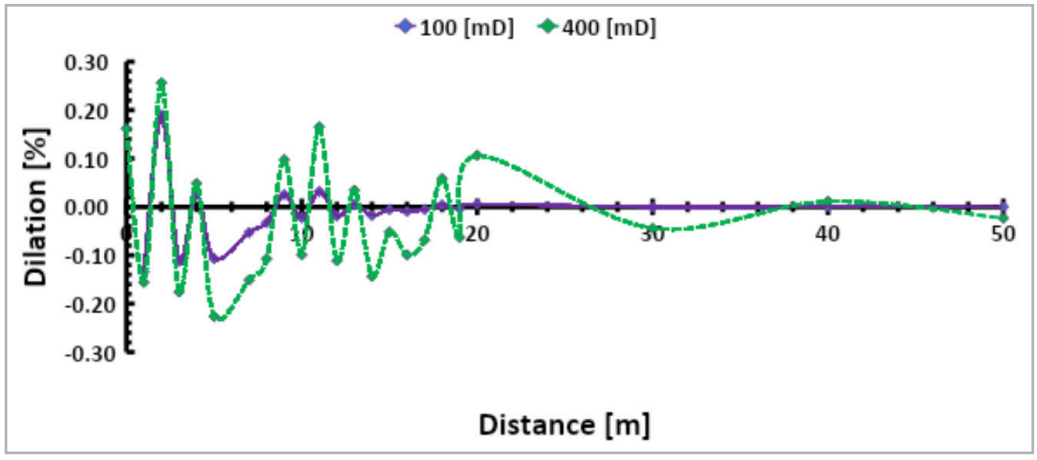

Figure 10. Illustrates the deformation caused by wave induction at two different permeabilities, where it can be observed that higher permeability results in a greater wave amplitude, indicating a larger sweep of the zone. Furthermore, higher permeability leads to a greater extent of dilation.

The laboratory tests were carried out using a confined cylindrical sand core initially saturated with 100% brine. Subsequently, the brine is displaced with oil, the injection line is closed, and the production line is opened. Oil is produced and closed when it reaches the predetermined volume. The production time for the volume is recorded, and this procedure is repeated 50 times. Then, the same process is repeated, but with the induction of waves directly into the core, and the time is recorded with the exact objective 50 times. Finally, the production rate is calculated, and the results are analyzed, **Figure 11**.

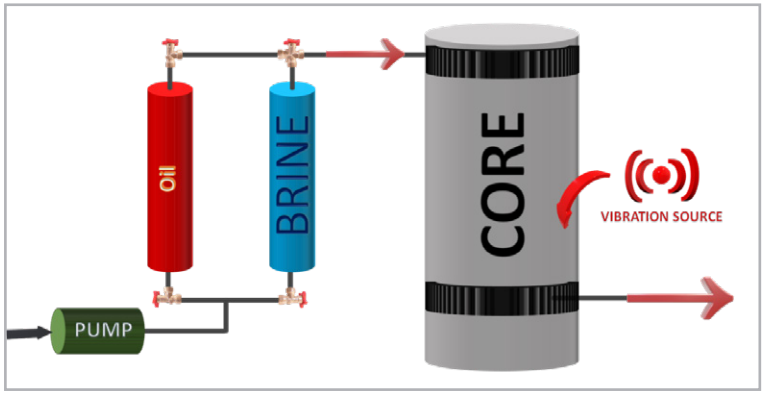

Figure 11. The laboratory tests for this work were conducted by inducing mechanical-vibratory waves (W/WAVES) directly into the core, thereby improving production compared to without wave (WO/WAVES) induction.

The lab report shows 100 displacements, 50 without induced waves (WO/WAVES) at 52.5 [BPD] rate, and 50 with induced waves (W/WAVES) at 126.5 [BPD] rate. The improved production rate can be observed at a ratio factor of 2.4 for this case, **Table 1**.

N°	q [BPD] WO/WAVES	q [BPD] W/WAVES	N°	q [BPD] WO/WAVES	q [BPD] W/WAVES
1	53. 3	106. 9	26	56. 6	115. 9
2	52. 2	121. 9	27	54. 0	112. 7
3	58. 6	122. 8	28	53. 3	107. 1
4	59. 2	116. 9	29	54. 4	129. 0
5	49. 1	124. 0	30	50. 8	127. 0
6	53. 1	129. 4	31	53. 2	114. 4
7	48. 7	136. 6	32	49. 0	112. 8
8	56. 5	111. 4	33	57. 0	122. 4
9	52. 8	110. 9	34	55. 6	132. 9
10	56. 0	127. 7	35	50. 8	140. 8
11	53. 8	133. 9	36	49. 5	144. 0
12	54. 6	126. 7	37	49. 0	117. 7
13	56. 6	135. 9	38	48. 6	111. 8
14	53. 3	143. 0	39	55. 6	136. 6
15	54. 5	143. 2	40	56. 7	141. 5
16	52. 3	123. 3	41	55. 4	150. 9
17	52. 7	127. 3	42	55. 5	140. 4
18	51. 1	123. 1	43	49. 7	121. 0
19	52. 2	118. 0	44	48. 8	114. 8
20	59. 3	112. 7	45	50. 5	109. 2
21	49. 8	123. 2	46	49. 1	135. 0
22	49. 5	129. 0	47	50. 3	150. 0
23	56. 1	128. 2	48	48. 5	137. 6
24	52. 2	136. 7	49	49. 1	126. 7
25	48. 6	145. 7	50	49. 4	113. 2

Table 1. The porous media used was unconsolidated sand cores (from Tláhuac mines, Mexico City).

In the laboratory tests, the deformation of the porous medium was carried out on pressurized packed sand cores with the following characteristics: ϕ = 0.2 (average), k = 1.7 [Darcys] (average), and μ_f = 0.064 [cp]. As observed in the previous results, dilation is measured by the pressure increase within the system, which results in an increase in production. **Figure 12** shows the expansion-contraction induced by the 350 [Hz] wave propagation in the cores.

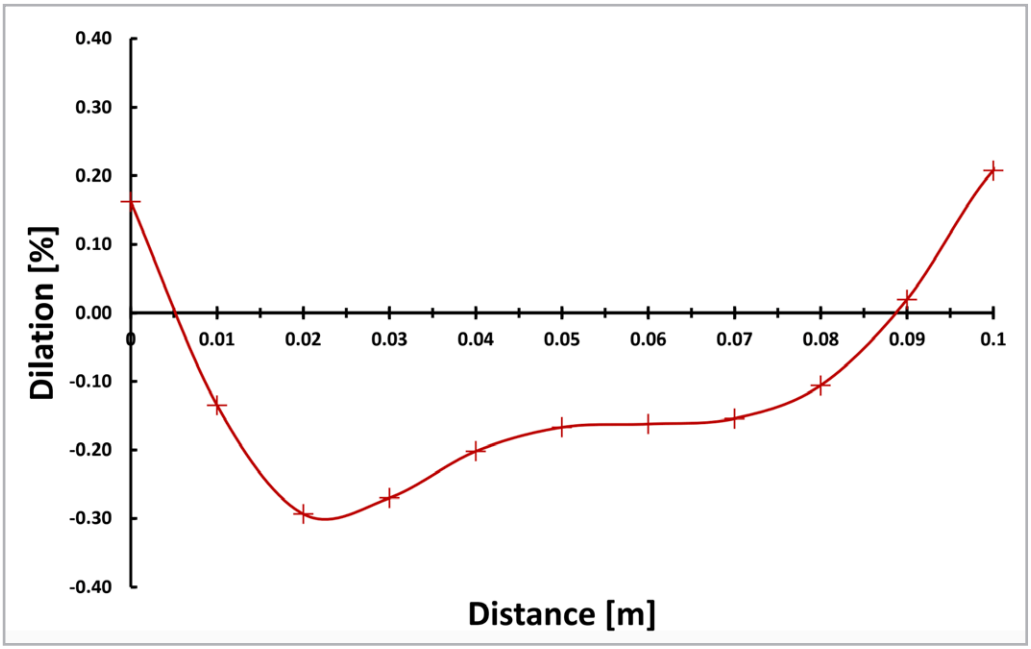

Figure 12. Illustrates the expansion of the porous medium in the laboratory core, which occurred at a frequency of 350 [Hz] and a distance of 0.1 [m]. This expansion caused an increase in pressure and immediate expulsion of the fluid contained, leading to a boost in production.

Figure 13 shows the cumulative production due to wave induction as a function of the sweep distance. The ordinate at the origin represents the original production (WO/WAVES). The cumulative production up to 0.1 [m] is the increase in production achieved by wave induction; it can be observed that it differs by 3.15 [%] from the mathematical model in the laboratory report. Therefore, the model is validated through these results.

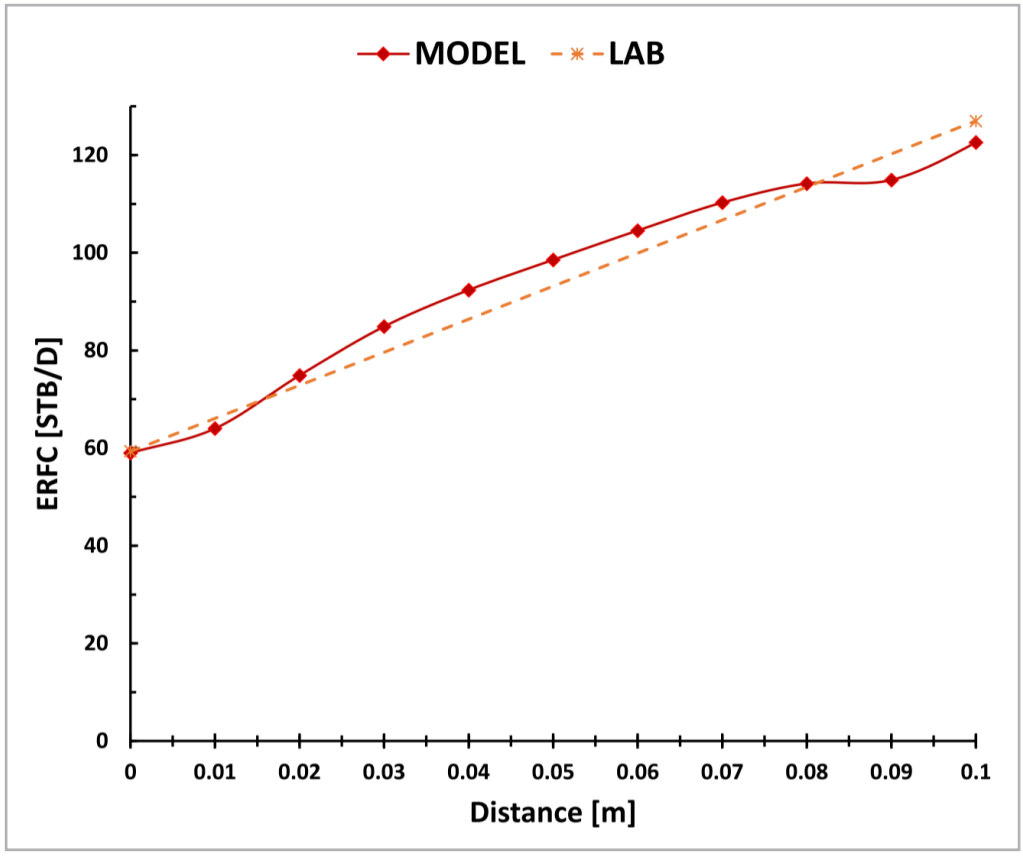

Figure 13. Enhancement of reservoir's flow capacity in the lab's core of length 0.1 [m]. The results indicate that the model used in the laboratory report is validated, as it differs by only 3.15 [%] from the observed increase in production, 127_{Lab} [BPD], 123_{Lab} [BPD].

Conclusions

- Induced mechanical waves (vibrations) increase the well rate.
- The general new model for harnessing wave induction in porous media was introduced.
- The mathematical model was validated based on laboratory tests with an error of 3.15 [%].
- The properties of the porous medium determine wave sweep, with attenuation indicating applicability barriers. Application depends on permeability, porosity, and the dynamic viscosity of the fluid.
- The wave sweep simulation up to 30 [m] for a reservoir for = 0.25, μ_f = 1 [cp], and k = 400 [md], reports an increase in production of 1080 [STB/D] using this method.

Nomenclature

a	=	s function [dl]
A_T	=	Cross-sectional area,[m^2,cm^2]
c	=	Wave velocity, $[\frac{m}{s}]$
c_1	=	Constant One of integration, [dl]
c_2	=	Constant two of integration, [dl]
c_f	=	Formation Compressibility, [psi^{-1}, Pa^{-1}]
e	=	Fluid dilation
e_{max}	=	Maximum Dilation Fluid, [dl]
f	=	Frequency,$\left[\frac{1}{s}, Hz\right]$
g	=	Local acceleration, $\left[\frac{ft}{s^2}\right]$

G = Solid shear modulus, psi
k = Permeability, [md]
K = Bulk Modulus , [Pa, psi]
k_{il} = Permeability tensor, [mD]
k_{wd} = Displacement coefficient, [dl]
L_{core} = Core Length [m]
N_{UE} = Normalized number, [dl]
N_{WTN} = Wave transmission numbers, [dl]
p = System pressure, [Pa]
p_f = Fluid pressure, [psi]
q = Production Rate ,$\left[\frac{m^3}{s}, STB/D\right]$
q_{ERFC} = Production Rate due to Enhanced Reservoir Flow Capacity,$\left[\frac{m^3}{s}, STB/D\right]$
r = Propagation radius, [m]
r_D = Dimensionless radius, [dl]
r_{drn} = Drainage radius, [m]
r_{src} = Wave Propagation Source Radius, [m]
s = Laplace´s constant, [dl]
t = Time, [s]
t_D = Dimensionless time, [dl]
t_{ind} = Induced time, [dl]
t_{nat} = Natural time, [dl]
u = Laplace´s variable, [dl]
$u_{i,j,k}$ = Vector Displacement, [dl,m,cm]
u_{0x} = Reference displacement, [m]
U = Vector Displacement, [dl,m,cm]
U_{Df} = Dl fluid wave displacement, [dl]
$\bar{U}_{Df}$ = Dl fluid wave Laplace domain displacement, [dl]
U_{Ds} = Dl solid wave displacement, [dl]
$\bar{U}_{Ds}$ = Dl solid wave Laplace domain displacement, [dl]
w_{fi} = Fluid displacement vector, [m]
w_{fl} = Fluid displacement vector, [m]
w_{si} = Solid displacement vector, [m]
w_{sl} = Solid displacement vector, [m]
x = Distance, [m]
x_e = Reference distance, [m]
x_D = Dimensionless distance, [dl]
x_i = Distance on i's coordinate, [m]
y = y-axis Direction, [dl]
z = Elevation, z-axis m, [dl]
α = Compresibility ratio, [dl]
β = Propagation term, $\left[\frac{1}{m}\right]$
γ = Shear Displacement, [m,cm,dl]
$\in$ = Rock dilation, [dl]
$\in_{max}$ = Maximum rock dilation, [dl]
η = Hydraulic diffusivity, $\left[\frac{m^2}{s}\right]$
η_{Diw} = Dl hydraulic diffusivity due to induced waves, [dl]
θ = Propagation term, [Hz]
λ = Lamé's Second Parameter, [Pa, psi]
μ = Fluid viscosity, [cp]
μ_f = Fluid viscosity, [cp]
ρ_f = Fluid density, $\left[\frac{Kg}{m^3}\right]$
ρ_s = Rock density, $\left[\frac{Kg}{m^3}\right]$
σ_{sji} = Stress tensor, [psi]
$\sigma_{i,j,k,t}$ = Stress tensor, [psi,Pa]
ϕ = Porosity, [dl]
ω_D = Dl wave frequency, [dl]
ω_f = Fluid wave displacement, [m]
ω_s = Solid wave displacement, [m]

References

1. Allen, N. F., Woods, R. D., and Richart, F. E. 1980. Fluid Wave Propagation in Saturated and Nearly Saturated Sands. *Journal of the Geotechnical Engineerig Division, ASCE* **106** (3): 235-254. https://doi.org/10.1061/AJGEB6.0000931.

2. Ariadji, T. 2005. Effect of Vibration on Rock and Fluid Properties: On Seeking the Vibroseismic Technology Mechanisms. Paper presented at the SPE Asia Pacific Oil and Gas Conference and Exhibition, Jakarta, Indondesia, April 5-7. SPE 93112. https://doi.org/10.2118/93112-MS.

3. Auriault, J. L., Lebaigue, O., and Bonnet, G. 1989. Dynamics of Two Immiscible Fluids Flowing through Deformable Porous Media. *Transport in Porous Media* **4**: 105-128. https://doi.org/10.1007/BF00134993.

4. Ba, J., Ma, R., Carcione, J. M. et al. 2019. Ultrasonic Wave Attenuation Dependence on Saturation in Tight Oil Siltstones. *Journal Petroleum Science and Engineering* **179** (August): 1114-1122. https://doi.org/10.1016/j.petrol.2019.04.099.

5. Basak, P., and Madhav, M. R. 1978. Effect of the Inertia Term in One-Dimensional Fluid Flow in Deformable Porous Media. *Journal of Hydrology* **38** (1-2): 139-146. https://doi.org/10.1016/0022-1694(78)90138-5.

6. Bear, J., and Corapcioglu, M. Y. 1989. Wave Propagation in Saturated Porous Media-Governing Equations. International Symposium on Wave Propagation in Granular Media, ASME Winter Annual Meeting.

7. Bear, J., and Corapcioglu, M. Y., eds. 1991. *Transport Processes in Porous Media*. Dordrecht: Springer-Science+Bussines Media. https://doi.org/10.1007/978-94-011-3628-0.

8. Bear, J. 2018. *Modeling Phenomena of Flow and Transport in Porous Media*. Cham, Switzerland: Springer. https://doi.org/10.1007/978-3-319-72826-1.

9. Berryman, J. G. 1981a. Elastic Wave Propagation in Fluid-Saturated Porous Media. *Journal of the Acoustical Soc*iety of *America* **69**: 416-424. https://doi.org/10.1121/1.385457.

10. Berryman, J. G. 1981b. Elastic Wave Propagation in Fluid-Saturated Porous Media II. *Journal of the Acoustical Soc*iety of *America* **70** (6): 1754-1756. https://doi.org/10.1121/1.387193.

11. Berryman, J. G. 1986. Elastic Wave Attenuation in Rocks Containing Fluids. *Applied Physics Letters* **49** (10): 552-554. https://doi.org/10.1063/1.97092.

12. Berryman, J. G. 1988. Seismic Wave Attenuation in Fluid-Saturated Porous Media. In *Scattering and Attenuations of Seismic Waves, Part I*, eds. K. Aki, R. S. Wu, 423-432. Basel: Birkhäuser. https://doi.org/10.1007/978-3-0348-7722-0_21.

13. Biot, M. A. 1956a. Theory of Propagation of Elastic Wave in a Fluid-Saturated Porous Solid. I. Low Frequency Range. *Journal of the Acoustical Society of Am*erica **28** (2): 168-178. https://doi.org/10.1121/1.1908239.

14. Biot, M. A. 1956b. Theory of Propagation of Elastic Waves in a Fluid-Saturated Porous Solid. II. Higher Frequency Range. *Journal of the Acoustical Society of Am*erica **28** (2): 179-191. https://doi.org/10.1121/1.1908241.

15. Biot, M. A. 1962a. Generalized Theory of Acoustic Propagation in Porous Dissipative Media. *Journal of the Acoustical Society of Am*erica **34** (9A): 1254-1264. https://doi.org/10.1121/1.1918315.

16. Biot, M. A. 1962b. Mechanics of Deformation and Acoustic Propagation in Porous Media. *Journal of Applied Physics* **33** (4): 1482-1498. https://doi.org/10.1063/1.1728759.

17. Brutsaert, W. 1964. The Propagation of Elastic Waves in Unconsolidated Unsaturated Granular Mediums. *Journal of Geophysical Research* **69** (2): 243-257. https://doi.org/10.1029/JZ069i002p00243.

18. Chen, A. H. D. 1986. Effect of Sediment on Earthquake-Induced Reservoir Hydrodynamic Response. *Journal of Engineering Mechanics, ASCE* **112** (7): 654-663. https://doi.org/10.1061/(ASCE)0733-9399(1986)112:7(654).

19. Chen, X., Zhong, W., He, Z. et al. 2016. Frequency-Dependent Attenuation of Compressional Wave and Seismic Effects in Porous Reservoirs Saturated With Multi-Phase Fluids. *Journal Petroleum Science and Engineering* **147** (November): 371-380. https://doi.org/10.1016/j.petrol.2016.08.031.

20. Choon, T. W., Aik, L. K., Aik, L. E. et al. 2012. Investigation of Water Hammer Effect through Pipeline System. *International Journal on Advanced Science, Engineering and Information Technology* **2** (3): 246-251. https://doi.org/10.18517/ijaseit.2.3.196.

21. Corapcioglu, M. Y., and Tuncay, K. 1996. Propagation of Waves in Porous Media. In *Advances in Porous Media*, ed. M. Y. Corapcioglu, Chap. 5, 361-440. Amsterdam: Elsevier.

22. Davidson, B. C., Dusseault, M. B., and Spanos, T. J. T. 1997. Comments on the Mechanisms Responsible for Pressure Pulse Enhancement of Fluid Flow in Oil Reservoirs. PE-TECH Inc. Internal Document.

23. Durgut, I., Gudmundsson, J. S., and Di Lullo, A. 2019. Investigating the Use of Pressure Pulses to Assess Near Wellbore Reservoir Parameters. *Selçuk Üniversitesi Mühendislik, Bilim Ve Teknoloji Dergisi* **7** (2): 331-345.

24. Dusseault, M., Davidson, B., and Spanos, T. 2000. Pressure Pulsing: The Ups and Downs of Starting a New Technology. *J Can Pet Technol* **39** (04): 13-17. PETSOC-00-04-TB. https://doi.org/10.2118/00-04-TB.

25. Favorskaya, A. V., and Petrov, I. B. 2016. Wave Responses from Oil Reservoirs in the Arctic Shelf Zone. *Doklady Earth Sciences* **466**: 214–217. https://doi.org/10.1134/S1028334X16020185.

26. Finjord, J. 1990. A Solitary Wave in a Porous Medium. *Transport in Porous Media* **5**: 591-607. https://doi.org/10.1007/BF00203330.

27. Garg, S. K. 1971. Wave Propagation Effects in a Fluid-Saturated Porous Solid. *Journal of Geophysical Research* **76** (32): 7947-7962. https://doi.org/10.1029/JB076i032p07947.

28. Garg, S. K., Brownell, D. H., Pritchett, J. W. et al. 1975. Shock-Wave Propagation in Fluid-Saturated Porous

Media. *Journal of Applied Physics* **46** (2): 702-713. https://doi.org/10.1063/1.321634.

29. Garg, S. K., and Nayfeh, A. H. 1986. Compressional Wave Propagation in Liquid and/or Gas Saturated Elastic Porous Media. *Journal of Applied Physics* **60** (9): 3045-3055. https://doi.org/10.1063/1.337760.

30. Gassman, F. 1951. Elastic Waves through a Packing of Spheres. *Geophysics* **16** (4): 673-685. https://doi.org/10.1190/1.1437718.

31. Geertsma, J. 1957. The Effect of Fluid Pressure Decline on Volume Changes of Porous Rocks. In *Transactions of the Society of Petroleum Engineers*, Vol. 210, SPE-728-G, 331-340. Richrdson, Texas, USA: Society of Petroleum Engineers. https://doi.org/10.2118/728-G.

32. Geertsma, J., and Smit, D. C. 1961. Some Aspects of Elastic Wave Propagation in Fluid Saturated Porous Solids. *Geophysics* **26** (2): 169-181. https://doi.org/10.1190/1.1438855.

33. Guo, X., Du, Z., Li, G. et al. 2004. High Frequency Vibration Recovery Enhancement Technology in the Heavy Oil Fields of China. Paper presented at the SPE International Thermal Operations and Heavy Oil Symposium and Western Regional Meeting, Bakersfield, California, USA, March 16-18. SPE-86956-MS. https://doi.org/10.2118/86956-MS.

34. Hardin, B. D., and Richart, F. E. 1963. Elastic Wave Velocities in Granular Soils. *Journal of the Soil Mechanics and Foundation Division, ASCE* **89** (1): 33-65. https://doi.org/10.1061/JSFEAQ.0000493.

35. Hong, S. J., Sandhu, R. S., and Wolfe, W. E. 1988. On Garg's Solution of Biot's Equations for Wave Propagation in a One-Dimensional Fluid Saturated Elastic Porous Solid. *International Journal for Numerical and Analytical Methods in Geomechanics* **12** (6): 627-637. https://doi.org/10.1002/nag.1610120605.

36. Hsieh, L., and Yew, C. H. 1973. Wave Motions in a Fluid-Saturated Porous Medium. *ASME. Journal of Applied Mechanics* **40** (4): 873-878. https://doi.org/10.1115/1.3423180.

37. Iida, K. 1938. The Velocity of Elastic Waves in Sand. *Bulletin of the Earthquake Research Institute, Tokio Imperial University* **16** (1): 131-144. https://gbank.gsj.jp/ld/resource/geolis/88820691.

38. Ishihara, K., Shimizu, K., and Yamada, Y. 1981. Pore Water Pressures Measured in Sand Deposits During an Earthquake. *Soils and Foundations* **21** (4): 85-100. https://doi.org/10.3208/sandf1972.21.4_85.

39. Jones, J. P. 1969. Pulse Propagation in a Poroelastic Solid. *ASME. Journal of Applied Mechanics* **36** (4): 878-880. https://doi.org/10.1115/1.3564789.

40. Kurawle, I., Kaul, M., Mahalle, N. et al. 2009. Seismic EOR—The Optimization of Aging Waterflood Reservoirs. Paper presented at the SPE Offshore Europe Oil and Gas Conference and Exhibition, Aberdeen, UK, September 8-11. SPE-123304-MS. https://doi.org/10.2118/123304-MS.

41. Lee, J. 1982. *Well Testing*, Vol. 1. Richardson, Texas, USA: SPE Textbook Series, Society of Petroleum Engineers.

42. Levin, M. P. 1996. On the Propagation of Pressure Waves in Saturated Porous Media. *Fluid Dynamics* **31**: 865–867. https://doi.org/10.1007/bf02030105.

43. Lévy, T. 1979. Propagation of Waves in a Fluid-Saturated Porous Elastic Solid. *International Journal of Engineering Science* **17** (9): 1005-1014. https://doi.org/10.1016/0020-7225(79)90022-3.

44. Madsen, O. S. 1978. Wave-Induced Pore Pressures and Effective Stresses in a Porous Bed. *Géotechnique* **28** (4): 377-393. https://doi.org/10.1680/geot.1978.28.4.377.

45. Matthews, C. S., and Russell, D. G. 1967. *Pressure Buildup and Flow Tests in Wells*, Vol. 1. Richardson, Texas, USA: SPE Monograph Series, Society of Petroleum Engineers.

46. Metzger, H. A. 1958. Preliminary Report on Fracturing by Vibration - A New Method of Well Stimulation. *J Pet Technol* **10** (11): 13-16. SPE-1107-G. https://doi.org/10.2118/1107-G.

47. Mynett, A. E., and Mei, C. C. 1983. Earthquake-Induced Stresses in a Poro-Elastic Foundation Supporting a Rigid Structure. *Géotechnique* **33** (3): 293-303. https://doi.org/10.1680/geot.1983.33.3.293.

48. Nabor, G. W., and Barham, R. H. 1964. Linear Aquifer Behavior. *J Pet Technol* **16** (05): 561–563. SPE-791-PA. https://doi.org/10.2118/791-PA.

49. Nikolaevskiy, V. N., Lopukhov, G. P., Liao, Y. et al. 1996. Residual Oil Reservoir Recovery With Seismic Vibrations. *SPE Prod & Fac* **11** (02): 89–94. SPE-29155-PA. https://doi.org/10.2118/29155-PA.

50. Pascal, H. 1986. Pressure Wave Propagation in a Fluid Flowing through a Porous Medium and Problems Related to Interpretation of Stoneley's Wave Attenuation in Acoustical Well Logging. *International Journal of Engineering Science* **24** (9): 1553-1570. https://doi.org/10.1016/0020-7225(86)90163-1.

51. Plona, T. J. 1980. Observation of a Second Bulk Compressional Wave in a Porous Medium at Ultrasonic Frequencies. *Applied Physics Letters* **36** (4): 259-261. https://doi.org/10.1063/1.91445.

52. Prevost, J. H. 1985. Wave Propagation in Fluid-Saturated Porous Media: An Efficient Finite Element Procedure. *International Journal of Soil Dynamics and Earthquake Engineering* **4** (4): 183-202. https://doi.org/10.1016/0261-7277(85)90038-5.

53. Raats, P. A. C., and Klute, A. 1969. Transport in Soils: The Balance of Momentum. *Soil Science Society America*

Journal **32** (4): 452-456. https://doi.org/10.2136/sssaj1968.03615995003200040013x.

54. Rangel Gutiérrez, M. U., Santamaría Díaz, E., Bautista Morales, R. et al. 2020. Induced Waves Well Testing. XXXV Jornadas Técnicas AIPM, CDMX, México, noviembre 27.

55. Rangel Gutiérrez, M. U., Samaniego Verduzco, F., Santamaría Diaz, J. E. et al. 2022. Inducción de Ondas Mecánicas como Método de Recuperación, como Proceso de Asistencia a los Distintos Métodos de Recuperación Conocidos, Solos o Combinados para el Aprovechamiento de la Producción de Hidrocarburos y para Fracturamiento en Yacimientos Petroleros (Número de solicitud MX/a/2022/015425). Fecha de presentación: 05/12/2022. Clasificación CIP: E21B 43/16; C09K 8/58. Clasificación CPC: E21B 43/16; C09K 8/58; C09K 8/584.

56. Richart, F. E., Hall, J. R., and Woods, R. D. 1970. *Vibrations of Soils and Foundations.* Englewood Cliffs, New Jersey: Prentice Hall.

57. Santos, J. E. 1986. Elastic Wave Propagation in Fluid-Saturated Porous Media. Part I: The Existence and Uniqueness Theorems. *ESAIM: Mathematical Modelling and Numerical Analysis* **20** (1): 113-128. https://doi.org/10.1051/m²an/1986200101131.

58. Santos, J. E., and Oreña, E. J. 1986. Elastic Wave Propagation in Fluid-Saturated Porous Media. Part II: The Galerkin Procedures. *ESAIM: Mathematical Modelling and* Numerical *Analysis* **20** (1): 129-139. https://doi.org/10.1051/m²an/1986200101291.

59. Santos, J. E., Douglas, J., Corberó, J. et al. 1990. A Model for Wave Propagation in a Porous Medium Saturated by a Two-Phase Fluid. *Journal of the Acoustical Society of Am*erica **87** (4): 1439-1448. https://doi.org/10.1121/1.399440.

60. Smith, P. G., and Greenkorn, R. A. 1972. Theory of Acoustical Wave Propagation in Porous Media. *Journal of the Acoustical Society of America* **52** (1B): 247-253. https://doi.org/10.1121/1.1913086.

61. Spanos, T., Davidson, B., Dusseault, M. et al. 2003. Pressure Pulsing at the Reservoir Scale: A New IOR Approach. *J Can Pet Technol* **42** (02): 16-28. PETSOC-03-02-01. https://doi.org/10.2118/03-02-01.

62. Spurk, H. J., and Aksel, N. 2008. *Fluid Mechanics*, second edition. Berlin: Springer. https://doi.org/10.1007/978-3-540-73537-3.

63. Sun, Q., Retnanto, A., and Amani, M. 2020. Seismic Vibration for Improved Oil Recovery: A Comprehensive Review of Literature. *International Journal of Hydrogen Energy* **45** (29): 14756-14778. https://doi.org/10.1016/j.ijhydene.2020.03.227.

64. Westermark, R. V., Brett, J. F., and Maloney, D. R. 2001. Enhanced Oil Recovery with Downhole Vibration Stimulation. Paper presented at the SPE Production and Operations Symposium, Oklahoma City, Oklahoma, USA, March 24-27. SPE-67303-MS. https://doi.org/10.2118/67303-MS.

Appendix A – Solution for the Closed Linear Reservoir Model

The dimensionless variables for the present problem are next defined:

Dimensionless time:

$$t_D = \frac{c}{X_e} t \qquad \text{(A. 1)}$$

Dimensionless solid wave displacement:

$$\omega_{Ds} = \frac{\omega_s}{u_{0x}} \qquad \text{(A. 2)}$$

Dimensionless fluid wave displacement:

$$\omega_{Df} = \frac{\omega_f}{u_{0x}} \qquad \text{(A. 3)}$$

Dimensionless distance:

$$X_D = \frac{X}{X_e} \quad \text{(A. 4)}$$

Wave transmission number:

$$N_{WTN} = \frac{c\,\tau_{WTN}}{X_e} \quad \text{(A. 5)}$$

Hydraulic diffusivity:

$$\eta = \frac{k_{il}G}{\mu\phi} \quad \text{(A. 6)}$$

Dimensionless hydraulic diffusivity due to induced waves:

$$\eta_{Diw} = \frac{\eta}{X_e c} \quad \text{(A. 7)}$$

Initial and boundary conditions Eqs. A.8 – A.11:

$$\omega_{Ds}\left(x_D, 0\right) = \omega_{Df}\left(x_D, 0\right) = 0; \quad \text{(A. 8)}$$

Wave condition Eqs. A.9 – A.11:

$$\frac{\partial \omega_{Ds}}{\partial t_D}\left(x_D, 0\right) = \frac{\partial \omega_{Df}}{\partial t_D}\left(x_D, 0\right) = 0; \quad \text{(A. 9)}$$

$$\omega_{Ds}\left(0, t_D\right) = \sin sin\, \omega_D t_D\,; \quad \text{(A. 10)}$$

$$\omega_{Ds}\left(x_D, t_D\right) = 0; \quad \text{(A. 11)}$$

Including the former considerations of this work, when employing dimensionless variables for Eqs. 1 and 2, the procedure is carried out as follows:

Wave propagation in the solid is described as follows:

$$\frac{\partial^2 U_{Ds}}{\partial X_D^{\,2}} = \frac{\partial^2 U_{Ds}}{\partial t_D^{\,2}} + \frac{1}{\eta_{Diw}} \frac{\partial\left(U_{Ds} - U_{Df}\right)}{\partial t_D} \tag{A. 12}$$

where, the fluid wave displacement in Laplace domain is:

$$\overline{U}_{Df} = \frac{\overline{U}_{Ds}}{sN_{WTN} + 1} \tag{A. 13}$$

Wave propagation within the fluid is:

$$\frac{\partial^2 U_{Df}}{\partial t_D{}^2} + \frac{1}{N_{WTN}} \frac{\partial\,(U_{Df} - U_{Ds})}{\partial t_D} = 0 \tag{A. 14}$$

Transforming Eqs. (A.14 and A.12) into Laplace domain:

$$S^2 \overline{U}_{Df} + \frac{s}{N_{WTN}}\,(U_{Df} - U_{Ds}) = 0 \tag{A. 15}$$

The Differential equation in Laplace domain results:

$$\frac{\partial^2 U_{Ds}}{\partial x_D{}^2} = S^2 \overline{U}_{Df} + \frac{s}{\eta_{Diw}}(u_{Ds} - u_{Df}) = S^2 \left\{1 + \frac{1}{s\eta_{Diw}}\left(1 - \frac{1}{sN_{WTN} + 1}\right)\right\} \bar{u}_{Ds} \tag{A. 16}$$

where, solid wave displacement in Laplace domain from Eq. (A.16) is:

$$\bar{u}_{Ds} = C_1 e^{(\sqrt{g(s)}\, s\, x_D)} + C_2 e^{(-\sqrt{g(s)}\, s\, x_D)} \tag{A. 17}$$

The solution of the solid wave displacement in Laplace domain:

$$\bar{u}_{Ds} = \frac{\omega_D}{\omega^2 + \omega_D{}^2} \frac{\cosh\left\{s\sqrt{g(s)}\,(1 - x_D)\right\}}{\cosh\left\{s\sqrt{g(s)}\right\}} \tag{A. 18}$$

where:

$$g(s) = \left\{1 + \frac{N_{WTN}}{\eta_{Diw}}\left(\frac{1}{sN_{WTN}+1}\right)\right\} \quad \text{(A. 19)}$$

Applying the inverse Laplace transformation for the solid wave displacement solution gives:

$$L^{-1}\{\overline{U}_{Ds}\} = U_{Ds} = \int_0^{t_D} \lambda \cos[\omega_D(t_D - \tau)]\left\{1 + \frac{4}{\pi}\sum_{n=1}^{\infty} C_n \cos\beta_n X \cos\beta_n \tau\right\} d\tau \quad \text{(A. 20)}$$

Applying the convolution integral to find the time-domain solution for wave propagation displacement in the fluid gives:

$$U_{Df} = \int_0^{t_D} \frac{1}{N_{WTN}} e^{-\left(\frac{t_D-\tau}{N_{WTN}}\right)} U_{Ds}(\tau) d\tau \quad \text{(A. 21)}$$

where

$$\beta_n = \left(\frac{2n-1}{2a}\right)\pi,\ a = \sqrt{g(s)}; \quad \text{(A. 22)}$$

At early time:

$$t_D \to 0\ \ a \to 1; \quad \text{(A. 23)}$$

At long time:

$$t_D \to \infty\ \ a = \left\{1 + \frac{N_{WTN}}{\eta_D}\right\}^{\frac{1}{2}} \quad \text{(A. 24)}$$

Finally, the solution for wave displacement in both phase is obtained from direct inversion of Eqs. A.20 and A.21:

$$U_{Ds} = \sin\omega_D t_D + \frac{4}{\pi}\sum_{1}^{\infty} \frac{\omega_D{}^2}{\omega_D{}^2 - \beta_n{}^2} C_n \cos\beta_n X \left[\sin\omega_D t_D - \frac{\beta_n}{\omega_D}\sin\beta_n t_D\right] \quad \text{(A. 25)}$$

The wave displacement in the fluid being:

$$U_{Df} = N_{UE}\left\{\omega_D N_{WTN} e^{-\frac{t_D}{N_{WTN}}} + \sin\omega_D t_D - \omega_D N_{WTN}\cos\omega_D t_D\right\} + \frac{4\omega_D}{\pi}\sum_{1}^{\infty}\frac{(-1)^n}{2n-1}\frac{\cos\left(\frac{2n-1}{2}\right)\pi[1-X_D]}{{\beta_n}^2+{\omega_D}^2}\left\{\omega_D N_{UE}\left(\omega_D N_{WTN} e^{-\frac{t_D}{NWT}} + \sin\omega_D t_D - \omega_D N_{WTN}\cos\omega_D t_D\right) - \frac{N_{WTN}\beta_n}{1+(\beta_n N_{WTN})^2}\left(\beta_n N_{WTN} e^{-\frac{t_D}{N_{WTN}}} + \sin\beta_n t_D - \beta_n N_{WTN}\cos\beta_n t_D\right)\right\} \quad \text{(A. 26)}$$

Appendix B - Solution for the Radial Closed Reservoir Model

The numerical solution of Eqs. 6 and 7 is presented in the following section, Eqs. B.1 and B.2 are solved through the finite difference method; the wave displacement in the solid is given by:

$$\omega_{Ds}(i,k) = \left(1 - \varphi_4\right)\omega_{Df}(i-1,k+1) - \omega_{Df}(i-1,k) + 2\,\varphi_4 * \omega_{Df}(i-1,k) - \varphi_4 * \omega_{Df}(i-1,k-1) + \omega_{Ds}(i,k-1) \quad \text{(B. 1)}$$

Finite differences for wave displacement in the fluid being:

$$\omega_{\mathrm{Df}}(\mathrm{i},\mathrm{k}) = \left\{\frac{\omega_{\mathrm{Df}}(\mathrm{i}+1,\mathrm{k}-1)+\omega_{\mathrm{Df}}(\mathrm{i}-1,\mathrm{k}-1)}{2} + \omega_{\mathrm{Ds}}(\mathrm{i},\mathrm{k}-1) * \left(\frac{\varphi_3}{2}-\varphi_2\right) + \omega_{\mathrm{Ds}}(\mathrm{i}-1,\mathrm{k}-1) * \left(\frac{\varphi_2}{2}-\frac{\varphi_3}{2}\right) + \omega_{\mathrm{Ds}}(\mathrm{i}+1,\mathrm{k}-1) * \left(\frac{\varphi_2}{2}-\frac{\varphi_1}{2}\right) - \frac{\varphi_1}{2}[\omega_{\mathrm{Df}}(\mathrm{i}-1,\mathrm{k}+1) - 2\,\omega_{\mathrm{Ds}}(\mathrm{i},\mathrm{k})]\right\} \quad \text{(B. 2)}$$

where:

$$R = \frac{{\Delta t_D}^2}{{\Delta r_D}^2} r_D \quad \text{(B. 3)}$$

$$\varphi_1 = \frac{\eta_D}{N_{WTN}} \quad \text{(B. 4)}$$

$$\varphi_2 = \frac{R\,\eta_D}{N_{WTN}} \quad \text{(B. 5)}$$

$$\varphi_3 = \frac{R\,\eta_D\,\Delta r_D}{N_{WTN}\,r_D} \quad \text{(B. 6)}$$

$$\varphi_4 = \frac{N_{WTN}}{\Delta t_D} \quad \text{(B. 7)}$$

Dimensionless radius is defined as the ratio of the difference between the propagation radius and the initial source radius, that is, from the wellbore face into the porous medium, with the limit of the drainage radius of the reservoir:

$$r_D = \frac{r - r_{src}}{r_{drn}} \quad \text{(B. 8)}$$

Appendix C – Vibratio – Permatio Model

For Biot's formulation for stress-strain relationships for a fluid saturated elastic porous medium, the components of the strain tensor of the solid matrix are:

$$\epsilon_{xx} = \frac{\partial u_x}{\partial x}, \quad \epsilon_{yy} = \frac{\partial u_y}{\partial y}, \quad \epsilon_{zz} = \frac{\partial u_z}{\partial z} \quad \text{(C. 1)}$$

$$\gamma_{xy} = \frac{\partial u_x}{\partial y} + \frac{\partial u_y}{\partial x}, \quad \gamma_{xz} = \frac{\partial u_z}{\partial x} + \frac{\partial u_x}{\partial z}, \quad \gamma_{yz} = \frac{\partial u_y}{\partial z} + \frac{\partial u_z}{\partial y} \quad \text{(C. 2)}$$

The dilation of rock (ϵ) is expressed in terms of displacement vector ($u_{i,j,k}$) as:

$$\epsilon = \nabla \cdot \mathrm{u_{i,j,k}} \quad \text{(C. 3)}$$

Assuming irrotational rock strain, the components of strain tensor of the fluid are:

$$\mathrm{e_{xx}} = \frac{\partial \mathrm{U_x}}{\partial \mathrm{x}}, \quad \mathrm{e_{yy}} = \frac{\partial \mathrm{U_y}}{\partial \mathrm{y}}, \quad \mathrm{e_{zz}} = \frac{\partial \mathrm{U_z}}{\partial \mathrm{z}} \quad \text{(C. 4)}$$

$$\gamma_{xy} = \frac{\partial \mathrm{U_x}}{\partial \mathrm{y}} + \frac{\partial \mathrm{U_y}}{\partial \mathrm{x}}, \quad \gamma_{xz} = \frac{\partial \mathrm{U_z}}{\partial \mathrm{x}} + \frac{\partial \mathrm{U_x}}{\partial \mathrm{z}}, \quad \gamma_{yz} = \frac{\partial \mathrm{U_y}}{\partial \mathrm{z}} + \frac{\partial \mathrm{U_z}}{\partial \mathrm{y}} \quad \text{(C. 5)}$$

The dilation of the fluid (e) is expressed in terms of the displacement vector (*U*) as:

$$e = \nabla \cdot U \quad \text{(C. 6)}$$

It should be pointed out that this expression is not the actual strain in the fluid, but simply the divergence of the fluid displacement, which itself is derived from the average volume flow through the pores (Corapcioglu and Tuncay, 1996).

Assuming the shear fluid stress is considered with the dynamic viscosity of the fluid.

Following Biot 1956, Corapcioglu and Tuncay 1996, assuming the solid skeleton of porous media is isotropic and for the relatively small deviations, it is perfectly elastic. The stress – strain relationships are expressed by:

$$\sigma_{xx} = 2G\epsilon_{xx} + \lambda\epsilon + Qe \quad \text{(C. 7)}$$

$$\sigma_{yy} = 2G\epsilon_{yy} + \lambda\epsilon + Qe \quad \text{(C. 8)}$$

$$\sigma_{zz} = 2G\epsilon_{zz} + \lambda\epsilon + Qe \quad \text{(C. 9)}$$

where:

$$\epsilon = \epsilon_{xx} + \epsilon_{yy} + \epsilon_{zz} \quad \text{(C. 10)}$$

The geomechanical terms for the determination of the resultant stress in fluid (Eq. C.12) and rock (Eq. C.11) dilation:

$$\lambda = \frac{\frac{\gamma}{K + \phi^2} + \alpha(1 - 2\phi)}{\gamma + \alpha \cdot c_f} - \frac{2G}{3} \quad \text{(C. 11)}$$

$$Q = \frac{\phi(\alpha - \phi)}{\gamma + \alpha \cdot c_f} \quad \text{(C. 12)}$$

where:

$$\alpha = 1 - \frac{c_f}{K} \quad \text{(C. 13)}$$

Dilations of the rock (Eq. C.14) and fluid (Eq. C.15) as a result of wave induction, exclusively considering the term related to wave propagation (Corapcioglu and Tuncay, 1996):

$$\epsilon = C_1 \cdot e^{i(\beta + \theta t)} \quad \text{(C. 14)}$$

$$e = C_2 \cdot e^{i(\beta + \theta t)} \quad \text{(C. 15)}$$

Dilations of the rock (Eq. C.16) and the fluid (Eq. C.17) considering the term related to wave attenuation:

$$\epsilon = \epsilon_{max} \cdot e^{i(\beta + \theta t)} e^{-(b)} \quad \text{(C. 16)}$$

$$e = e_{max} \cdot e^{i(\beta + \theta t)} e^{-(b)} \quad \text{(C. 17)}$$

where attenuation term (Corapcioglu and Tuncay, 1996):

$$b = \frac{\mu_f \cdot \phi^2}{k} \quad \text{(C. 18)}$$

and propagation terms (Corapcioglu and Tuncay, 1996):

$$\beta = \frac{\omega}{v} \quad \text{(C. 19)}$$

$$\theta = \omega = 2 \cdot \pi \cdot f \quad \text{(C. 20)}$$

The stress in the fluid (σ), is proportional to the fluid pressure (p) by (Corapcioglu and Tuncay, 1996):

$$-\sigma = \phi \cdot p \quad \text{(C. 21)}$$

For all directions:

$$-\nabla\sigma = \phi \cdot \nabla p \quad \text{(C. 22)}$$

Darcy's Law:

$$q = -\frac{k \cdot \phi \cdot A_T}{\mu_f} \frac{dp}{dx} \quad \text{(C. 23)}$$

Modifying Darcy's Law for quantifying the production due to induced waves for one direction:

$$q_{ERFC} = \frac{k \cdot A_T}{\mu_f} \sigma_{xx} \quad \text{(C. 24)}$$

Or

$$q_{ERFC} = \frac{k \cdot A_T}{\mu_f} \left[\epsilon_{max} \cdot e^{i(\beta + \theta t)} e^{-(b)} (2G + \lambda) + Q\, e_{max} \cdot e^{i(\beta + \theta t)} e^{-(b)} \right] \quad \text{(C. 25)}$$

The propagation was determined by solving Eqs. (1 and 2) and was used to solve Eq. (C.25), thus obtaining the complete solution.

Semblanza de los autores

Mario Ubaldo Rangel Gutiérrez

Obtuvo la Licenciatura en Ingeniería Petrolera en la Universidad Nacional Autónoma de México, y actualmente está completando su Maestría en ingeniería en la misma institución. Anteriormente, trabajó como Ingeniero de yacimientos para XPETRUS. Es profesor adjunto en la UNAM y actualmente se desempeña como consultor para Methane Storm Energy.

Fernando Samaniego Verduzco

Obtuvo el título de Licenciatura y Maestría en la Universidad Nacional de México y un Doctorado en la Universidad de Stanford, todos en Ingeniería Petrolera. Ha trabajado para el Instituto Mexicano del Petróleo, el Instituto de Investigaciones Eléctricas, PEMEX y actualmente es profesor emérito de Ingeniería Petrolera en la Universidad Nacional de Autónoma de México.

José Emilio Santamaría Díaz

Obtuvo una Licenciatura en Ingeniería Petrolera de la UNAM y recientemente en proceso de graduación de la Maestría en Ingeniería de Yacimientos en la Facultad de Ingeniería de la UNAM. Trabajó en la industria Upstream en servicios de pozos y operaciones de producción, y actualmente trabaja como Asistente Académico en la División de Ciencias de la Tierra en la UNAM.

Rafael Santamaría Díaz

Ingeniero Petrolero graduado por la Facultad de Ingeniería de la Universidad Nacional Autónoma de México, actualmente en proceso de obtener su Maestría en el programa de Exploración y Explotación de Recursos Naturales en la misma institución.

Reynaldo Bautista Morales

Obtuvo el título de Maestría en Ingeniería en Exploración y Explotación de Recursos Naturales de la Universidad Nacional Autónoma de México, bajo la supervisión del Dr. Fernando Samaniego Verduzco. Actualmente es aspirante al doctorado en la misma nstitución.